2023 IEEE International Conference on Robotics and Automation (ICRA 2023)
May 29 - June 2, 2023. London, UK

The Human Gaze Helps Robots Run Bravely and Efficiently in Crowds

Qianyi Zhang, Zhengxi Hu, Yinuo Song, Jiayi Pei, and Jingtai Liu, *Senior Member, IEEE*

***Abstract*—In human-aware navigation, the robot tacitly games with humans, balancing safety and efficiency according to human intentions. Poor balance or bad intent recognition causes the robot to stop conservatively or advance rashly, resulting in a deadlock or even a collision respectively. To address the issue, this paper proposes an improved limit cycle for collaboratively parameterizing human intentions and planning robot motions. The human-robot interaction is modeled as a dynamic chicken game with incomplete information, where the human gaze is introduced to depict the unique characteristics of each person, allowing the robot to approach with different safety margins. Our method is tested in challenging indoor scenarios and outperforms traditional methods in both safety and efficiency. We enable robots to utilize human wisdom to solve problems that cannot be solved on their own. The robot bravely goes through oncoming crowds by getting closer to people with higher attention on it and has the foresight to stably cross in front or behind people.**

I. Introduction

Planning for robots in crowds is challenging, as the physical space is compressed and robots must predict human behaviors [1]. Robots are required to yield to people appropriately for safety and to bravely go through crowds for efficiency. Classical approaches focus on the former. To keep robots safe from people, the human body is approximated as a cylinder and dilated by a safety margin, which is defined by Hayduk as personal space, a circle around the human that the robot should not invade [2]. Others improve the circle to ellipse [3], egg shape [4], asymmetric Gaussian distribution [5], etc. However, an overly conservative margin further compresses the planning space, making the robot tend to stop in the crowd to avoid collisions. Also, it can lead to the "frozen robot" problem, where the robot has no feasible trajectory to restart in a fast-moving crowd [6].

In fact, some margins are redundant and can be changed according to human attention. For example, people observing the robot will be more watchful, allowing the robot to approach them closer, but people playing with the phone will behave more unpredictably, requiring the robot to keep a greater distance. This is the central proposition of this paper: we introduce human gaze information [7] to identify human attention and then adaptively adjust the safety margin for everyone in the crowd, freeing up more viable space for robots to move through the crowd more bravely and efficiently.

The authors are with the Institute of Robotics and Automatic Information System, Nankai University, Tianjin, 300350, China. {zhangqianyi, hzx, 1810912, 2011737}@mail.nankai.edu.cn; liujt@nankai.edu.cn. This work is supported in part by National Key Research and Development Project under Grant 2019YFB1310604, in part by National Natural Science Foundation of China under Grant 62173189.

The interaction between humans and robots forms a game. Both of them pick strategies based on their predictions of how others will act. For the robot, the first challenge is to predict human favored strategies and find its optional strategies. Limit cycle [8] is introduced to solve this problem. It is a key notion in control theory that describes periodic systems that eventually revert to their original periodic states after being disrupted. Kim [9] originally used it in navigation because of its ability to direct an object to approach a circle. Then Lounis [10] utilized it to plan trajectories for mobile robots to avoid circular obstacles. They proposed elliptic limit cycle [11] and parallel elliptic limit cycle [12], and designed a special variable u to reflect the safe distance when the robot goes around the obstacle. Inspired by these works, we find that limit cycle has an inherent connection with human behavior prediction: (a) The bodies of humans and most service robots are roughly circular and can be seen as the center circle of limit cycle. (b) In the event of a probable collision, the human will not take a long detour but will pass by the robot with a certain safety margin and then go back to the original route, which is consistent with the limit cycle's characteristic of attracting objects to approach but not allowing them to collide. (c) The margin's size can be directly reflected on u. In this case, the limit cycle is introduced in this paper to parameterize human behavior and make joint strategies for both the human and the robot for the first time. It outperforms classic approaches [13], [14] in predicting human favored strategies. The robot behaves more understandably and predictably, allowing humans to quickly identify its decisions and react cooperatively.

The second challenge is to select the best strategy for the robot among options, considering the human-robot interaction in the future. We model the conflict between a person and a robot with a probable collision as a dynamic chicken game with incomplete information [15], the principle of which is that *while the ideal outcome is for one player to yield (to avoid the collision if neither yields), individuals try to avoid it out of pride for not wanting to look like a "chicken"* [16]. Both the human and the robot are assumed to follow Nash equilibrium strategies. The game starts from a loss-loss situation where a probable collision between the human and the robot exists. The robot guides the human to yield first by a specific number of tentative actions. If the human compromises, the robot wins. Otherwise, the robot will yield to the human to prevent the collision, and the human wins. During this process, the robot's optional strategies and the human favored strategies are estimated by an improved limit cycle, and the human gaze determines how

979-8-3503-2365-8/23/$31.00 ©2023 IEEE

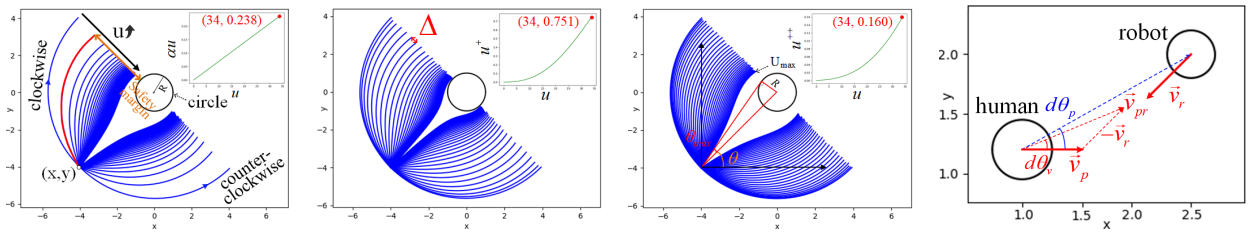

(a) Basic Limit Cycle (b) Gamma-resampled Limit Cycle (c) Improved Limit Cycle (d) Estimate Human Favored Direction

Fig. 1: The improved process of the limit cycle is shown in (a)-(c) where the trajectories are distributed more and more evenly. (d) shows an intuitive example of estimating the human favored direction as counter-clockwise.

much the robot should compromise with the human (safety margin's size). Even though several recent works [17]–[19] have dealt with human-robot interaction as a game, these works are all based on the pose (position plus orientation) information. It's commonly accepted [20] that pose is result-side information that records what has happened and infers the future with inertia. It lags and only contains coarse future information. No matter how well designed an algorithm is, it cannot break through the limitations caused by the information source itself. In the contrast, the gaze information is cause-side information and inherently contains sufficient future information. Our work gives the robot additional information about human intent to assist it in making brave decisions and avoiding unnecessary yield.

In summary, our primary contributions are as follows:

- Propose an improved limit cycle to simultaneously parameterize human behavior and plan for the robot.
- Model human-robot interaction as a dynamic chicken game with incomplete information and introduce human gaze to adaptively adjust everyone's safety margin.

II. Parameterize Human Behavior by Limit Cycle

This section presents an improved limit cycle for estimating strategies for humans and robots. Based on human-robot interactions, the human favored strategy is predicted.

A. Preliminaries of Limit Cycle

The vector field defined by a limit cycle drives an object at (x, y) to a circle of radius R centered at the origin [10]:

$$F_x(x, y, R, dir, u) = dir \cdot y + u \cdot x \cdot (R^2 - x^2 - y^2) \quad (1)$$

$$F_y(x, y, R, dir, u) = -dir \cdot x + u \cdot y \cdot (R^2 - x^2 - y^2) \quad (2)$$

where the driving force is (F_x, F_y). $dir \in \{-1, 1\}$ denotes the direction during the approach (counter-clockwise or clockwise). The variable u balances the vector pointing to the origin ($u \to \infty$) with its perpendicular vector ($u \to 0$). Assuming the object moves n steps, a simulated trajectory τ is formed:

$$\tau(x, y, R, dir, u) = \{(x_i, y_i)|_{i \in [0,n] \wedge i \in \mathbb{N}}\} \quad (3)$$

The safety margin is the distance from the last point (x_n, y_n) to the human body. Fig.1(a) shows multiple simulated trajectories varied with dir and u. As u increases from 0 to U_{max} in integer, the safety margin decreases.

B. Improvement of Limit Cycle

The first term in Equ.1-2 varies linearly along (x, y), while the second is quadratic, causing trajectories to be sparse at small u and redundantly pile up at large u. To distribute them evenly, Gamma distribution is designed to resample u:

$$u^+ = Gamma(u|\alpha, \beta) = \frac{\beta^\alpha \cdot u^{\alpha-1} e^{-\beta u}}{\Gamma(\alpha)} \quad (4)$$

where α and β are constant parameters. $\Gamma(\alpha) = (\alpha - 1)!$. Replacing u in Equ.1-2 with u^+, the trajectories in Fig.1(b) become more uniform, while some of them still pile up around the circle since the range of u^+ is too big on the domain $[0, Umax]$. An adaptive weakening coefficient α_{dis} entirely lowers them, satisfying the initial driving force of U_{max} tangent to the circle as shown in Fig.1(c). α_{dis} is figured out by the clockwise trajectory produced by α_{dis} and U_{max}:

$$U^{++}_{max} = Gamma(\alpha_{dis} \cdot U_{max}|\alpha, \beta) \quad (5)$$

$$tan(\theta + \theta_{max}) = \frac{F_y(x, y, R, 1, U^{++}_{max})}{F_x(x, y, R, 1, U^{++}_{max})} \quad (6)$$

C. Optional Strategies and Human Favorite Strategy

When there is a probable collision between a robot at state $X_r = (x_r, y_r, \dot{x}_r, \dot{y}_r, \theta_r, R_r)$ and a person at state $X_h = (x_h, y_h, \dot{x}_h, \dot{y}_h, \theta_h, R_h)$, both of them have to decide: which side to pass by each other (left or right), and how far to maintain (safety margin). Limit cycle solves the former by dir and the latter by u. As shown in Fig.1(d), the human can pass by the robot counter-clockwise ($dir = -1$) or clockwise ($dir = 1$) and his favored one can be estimated by comparing his orientation $d\theta_v$ and his relative direction to the robot $d\theta_p$:

$$dir^*_h = sign(d\theta_v - d\theta_p) \quad (7)$$

To estimate the human-favored safety margin, the robot of radius $R_h + R_r$ is taken as the origin, and the position of the human relative to the robot is $(\Delta x = x_h - x_r, \Delta = y_h - y_r)$. With the improved limit cycle, there are U_{max} optional strategies (safety margins) for each dir, and the human-favored strategy is the one with the minimum angular error:

$$u^*_h = \underset{u \in [0, U_{max}]}{\arg\min} \left| \frac{F_y(\Delta x, \Delta y, R_h + R_r, dir^*_h, u)}{F_x(\Delta x, \Delta y, R_h + R_r, dir^*_h, u)} - d\theta_v \right| \quad (8)$$

Correspondingly, when human-centered, the robot has $2 \times U_{max}$ optional strategies.

III. Gaze-Guided Human-Robot Game

This section describes the dynamic chicken game between the human and the robot. We start from a Crash-Crash situation and show how the robot guides the human to yield by tentative actions. Two Nash equilibriums are present where the robot picks its strategy according to the human strategy and gaze.

A. Dynamic Chicken Game Between Human and Robot

The two players in a chicken game are a person and a robot that may collide [21]. To avoid a collision, at least one player must yield to the other. Because the extra movement caused by yielding reduces efficiency (for example, detour to avoid oncoming people in a corridor), both players tend to continue forward and expect the other to yield. Eventually, at least one player will succumb to safety, resulting in higher payoffs for more aggressive players and fewer payoffs for more cautious players. So one transformation to end the game is from *Crash-Crash* to *H,Lose-R,Win* (human lose-robot win) or *H,Win,R,Lose* (human win-robot lose). Since neither player has any motivation to change their strategy (otherwise their payoff will be lower), nash equilibriums arise here and the game can end stably [22]. However, due to human uncertainty and sensor noise, two nash equilibriums can transform through *Tie-Tie*. Because *Tie-Tie* is an unstable temporal state, once the original equilibrium is broken, both players have strong motivations to converge the game from *Tie-Tie* to a new equilibrium in their favor.

human \ robot	Yield	Forward
Yield	Tie - Tie	H,Lose - R,Win
Forward	H,Win - R, Lose	Crash - Crash

Fig. 2: A payoff matrix of the chicken game.

B. Crash-Crash: Human Uncertainty and Tentative Actions

When a person and a robot are about to collide, the human does not clearly express his intention (strategy) to interact with the robot. Given that humans have full constraints and that human behavior prediction errors accumulate over time, a two-dimensional Gaussian distribution is used to model human uncertainty [5]. The normalized value represents the likelihood that the person will reach the position in the future:

$$G(\rho, \theta | \sigma_f, \sigma_{lr}) = e^{(-\frac{\rho^2 cos^2\theta}{2\sigma_f^2} - \frac{\rho^2 sin^2\theta}{2\sigma_{lr}^2})} \tag{9}$$

where (ρ, θ) is a point in the polar coordinate system with the robot as the origin. σ_f and σ_{lr} are longitudinal and later variances respectively.

In order for human beings to clearly express their intentions, and for the game to enter a nash equilibrium as soon as possible, small tentative actions are executed by the robot to guide human movements. This action is one of the strategies

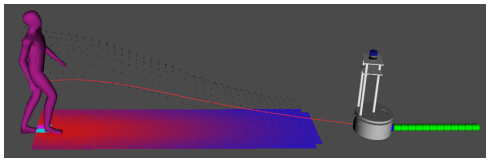

Fig. 3: Human uncertainty and the robot's tentative action.

from improved limit cycle, which requires the robot to avoid the human for safety and approach its goal $\mathcal{G}$ for efficiency:

$$J_r(dir, u) = -w_1 \max_{i=0}^{n} G(\tau.i(u)) - w_2 ||\tau.n(u) - \mathcal{G}||_2 \tag{10}$$

$$dir_r^*, u_r^* = \underset{u \in [0, U_{max}] \wedge u \in \mathbb{N}, dir \in \{-1,1\}}{\arg\max} J_r(dir, u) \tag{11}$$

where w_1 and w_2 are constant parameters, τ is a trajectory generated by improved limit cycle, and $\tau.i$ is the i^{th} point.

C. H,Win-R,Lose: Yield to Humans According to Attentions

If the person insists on continuing forward after a certain number of attempts, the robot compromises, and the game reaches a *H,Win-R,Lose* situation. But if the person moves cooperatively, the robot wins and can pass by the human more efficiently. The human choice is evaluated using the following criteria: recalling the tangent design in improved

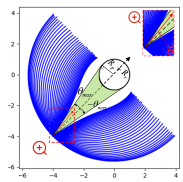

(a) Human choice identification

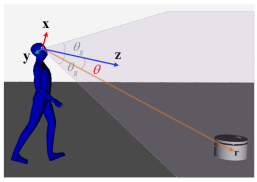

(b) Human attention to the robot

Fig. 4: Elements in *H,Win-R,Lose* situation.

limit cycle, when the human orientation falls within the green zone bounded by θ_{max} and $-\theta_{max}$ in Fig.4(a), there is no proper u to estimate the human-favored strategy due to the error between the estimated and the real orientations being too large. The person is considered to be aggressive and the *H,Win-R,Lose* equilibrium is reached.

The robot changes from small tentative actions to yield actions adjusted according to the human's attention to the robot. We define the human's attention $\mathcal{A}(t)$ as the difference θ between the human's gaze direction $\vec{oz}$ and the robot's direction relative to the human $\vec{or}$ as Fig.4(b) shows. It decays over time and can be updated with a new glance:

$$\mathcal{A}(t|\alpha_g, \beta_g) = \begin{cases} \beta_g \mathcal{A}(t-1) & \theta > \theta_g \\ max(\alpha_g(\pi - \theta), \beta_g g(t-1)) & otherwise \end{cases} \tag{12}$$

where $g(0) = 0$. α_g and β_g are constant parameters. Human attention is reflected in human uncertainty. People who pay more attention to the robot have lower uncertainty, which allows the robot to get closer to it without collision:

$$\sigma_{lr}(t) = e^{-\mathcal{A}(t)} \tag{13}$$

D. H,Lose-R,Win: Trust Humans to behave Cooperatively

When a human performs cooperative actions, his strategy can be captured by improved limit cycle as u_h^* and dir_h^*. At this time, the robot wins and realizes that the human is willing to compromise with it. However, unlike the winner (human) in *H,Win-R,Lose* situation, the robot is not allowed to move greedily without considering obstacle avoidance in human-centered navigation. Our victory lies in that the robot can have a higher expectation of human concessions without having to take such a large detour as in the *H,Win-R,Lose* situation. A one-dimensional asymmetric Gaussian

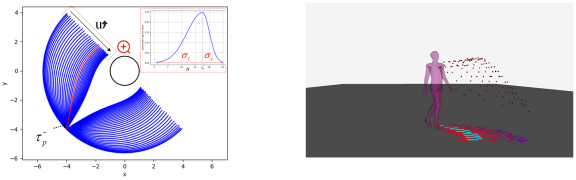

(a) Human strategy identification (b) Asymmetric Gamma distribution

Fig. 5: Elements in *H,Lose-R,Win* situation.

distribution is designed to reflect this expectation:

$$AG(u_h|u_h^*,\sigma_l,\sigma_r) = \begin{cases} e^{\frac{-(u_h-u_h^*)^2}{2\sigma_l^2}} & u_h <= u_h^* \\ e^{\frac{-(u_h-u_h^*)^2}{2\sigma_r^2}} & u_h > u_h^* \end{cases} \tag{14}$$

where u is asymmetrically distributed on both sides of u_h^*, σ_l and σ_r reflect the variances on the left and the right respectively. The expectation is influenced by human attention. A person who pays attention to the robot will be watchful, so that the robot can raise the expectation of human yielding, and can get closer to him if necessary. Whereas, a person who pays little attention to the robot but acts cooperatively has more confidence in the robot's obstacle avoidance ability. To live up to this trust, the robot must keep a further separation. In summary, the human payoff consists of the asymmetric Gaussian and the human-robot distance, while the robot expects to reach the goal quickly and keeps a safe distance. We collaboratively optimize their payoffs:

$$\begin{aligned} u_r^*, u_h^* = \arg\max_{u_r,u_h} [& w_3 AG(u_h|u_h^*,\sigma_l,\sigma_r) \\ & - w_4||\tau_r(u_r).n - \mathcal{G}||_2 + \alpha_d f_{dis}(u_h,u_r)] \end{aligned} \tag{15}$$

where w_3, w_4, and $\mathcal{D}$ are constant parameters. $\sigma_l = e^{dir_r^* g(t)}$, $\sigma_r = e^{-dir_r^* g(t)}$ and $\alpha_d = \mathcal{D} - \mathcal{A}(t)$ vary with $\mathcal{A}(t)$.

E. Workflow of Chicken Game with Gaze Guidance

The entire navigation process is described in Algorithm 1. If there is no potential collision, the robot follows the global plan (2-3). Otherwise, if there is a sufficient safety distance, the robot guides the human to cooperate by tentative actions (5-7). Then, the game enters a *H,Win-R,Lose* (11-14) or *H,Lose-R,Win* (15-19) situation according to the relative states of the human and the robot (9-10), where parameters are updated by gaze, human uncertainty is depicted by (asymmetric) Gauss distribution, and the robot's strategy is followed (22-23).

Algorithm 1: Navigation framework of CG3

Data: human states X_{list}, robot state X_r, camera image Img, global path τ_{global}
Result: Action to be performed by the robot (v, w)

1 $X_h \leftarrow detectCollision(X_{list})$;
2 **if** $X_h == None$ **then**
3 $\quad v, w \leftarrow trajFollower(\tau_{global})$
4 **else**
5 $\quad$ **if** $||X_h - X_r||_2 >= D_{safe}$ **then**
6 $\quad\quad G \leftarrow fitGauss()$;
7 $\quad\quad dir_r^*, u_r^* \leftarrow Crash\text{-}Crash(X_h, X_r, G)$;
8 $\quad$ **else**
9 $\quad\quad \mathcal{A}(t) \leftarrow updateAttention(Img)$;
10 $\quad\quad dir_h^*, u_h^* \leftarrow estimateStrategy(X_h, X_r)$;
11 $\quad\quad$ **if** $u_h^* == None$ **then**
12 $\quad\quad\quad \sigma_{lr}(t) \leftarrow updateParam(\mathcal{A}(t))$;
13 $\quad\quad\quad G \leftarrow fitGauss(\sigma_{lr}(t))$;
14 $\quad\quad\quad dir_r^*, u_r^* \leftarrow H,Win\text{-}R,Lose(X_h, X_r, G)$;
15 $\quad\quad$ **else**
16 $\quad\quad\quad \sigma_l, \sigma_r, \alpha_d \leftarrow updateParams(\mathcal{A}(t))$;
17 $\quad\quad\quad AG \leftarrow fitAsyGauss(\sigma_l, \sigma_r, \alpha_d)$;
18 $\quad\quad\quad u_r^*, u_h^* \leftarrow H,Lose\text{-}R,Win(X_h, X_r, AG)$;
19 $\quad\quad\quad dir_r^* \leftarrow dir_h^*$;
20 $\quad\quad$ **end**
21 $\quad$ **end**
22 $\quad \tau_r^* \leftarrow formTraj(dir_r^*, u_r^*, X_h, X_r)$;
23 $\quad v, w \leftarrow trajFollower(\tau_r^*)$;
24 **end**

IV. Simulation and Experiment

This section applies our approach (Chicken Game with Gaze Guidance, CG3) to passing and crossing scenarios [23]. We first verify the ability improved limit cycle to uniformly distribute trajectories and estimate human strategies. CG3 is then tested in two passing scenarios to show how the human gaze affects the robot's decision-making, and it is compared with a classic method (Timed Elastic Band, TEB) [24] in more challenging scenarios to demonstrate its high efficiency. The robot used in the experiment is a two-wheel differential robot. The gaze recognition method comes from an open-source work [7]. A probable collision exists when the distance between two future trajectories is less than 0.2 meters. The trajectory follower is Model Predictive Control.

A. Performance of Human Strategy Estimation

We operate the robot to interact with people in 3 real-world scenarios: (a) Ask people to walk forward in the middle of the corridor and return to the middle after a brief interaction with a robot. (b) People walking out of doors accidentally encounter the robot and detour to avoid it. (c) People cross a robot at an intersection and select to pass in front or behind it. The human trajectories, human gazes, and robot odometers are recorded. Kalman filter(KF) [13], lattice plan with Bayesian inference(LPBI) [14], and our approach (improved limit cycle) are compared to estimate human

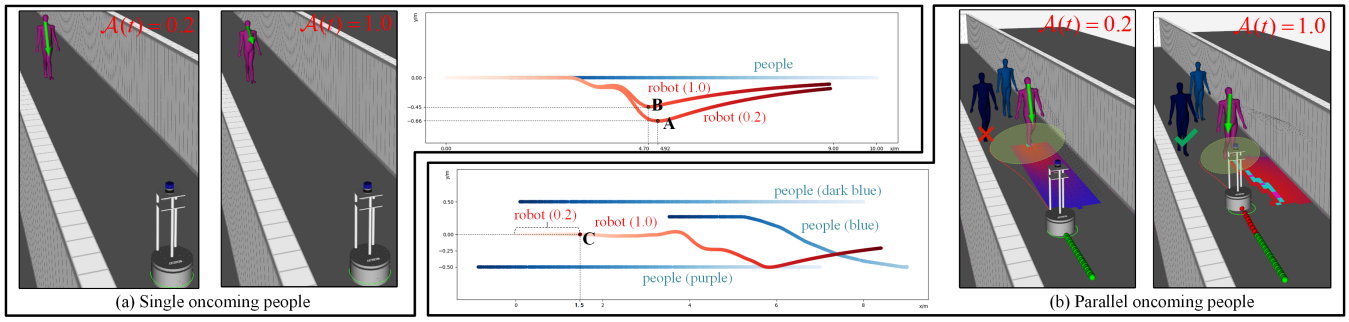

Fig. 6: *Single* and *parallel* scenarios. The robot estimates human safety margins and makes decisions according to human attentions $\mathcal{A}(t)$. For more details, visit: https://youtu.be/q60r3eQVfio

strategies (trajectories). The performances are evaluated by two commonly recognized measures: average distance error (ADE) and final distance error (FDE) [25]. ADE takes the average error between the prediction and the ground truth for the next five moments, and FDE takes just the fifth. Because people prefer to detour slightly and return to their original route when interacting with robots, consistent with the property of limit cycle that attracts objects to approach but does not allow them to reach, our method captures human strategies more accurately.

Moreover, to evaluate the performance of improved limit cycle on homogenizing the trajectory distribution, we compare the simulated trajectories generated by the original limit cycle and our improved limit cycle. The difference between adjacent safety margins as shown in Fig.1(b) with Δ is taken as a measure. Improved limit cycle has a smaller variance σ^2, which means the trajectory distribution is more uniform.

TABLE I: Compare Results

Method		ADE($/cm$)	FDE($/cm$)	$\sigma^2(/cm^2)$
LPBI		10.4	18.1	—
Kalman filter		4.1	7.0	—
Limit cycle	origin	4.4	7.9	24.87
	ours	2.5	5.0	0.86

B. Performance of Decision-making with Gaze Information

Single: Fig.6(a) shows the robot's performance in a passing scenario with one oncoming person. When a person lowers his head and plays with his phone (left), he only pays less attention to the robot and his future behaviors are more unpredictable. The robot is more inclined to safety. It believes that the person should be given a larger safety margin and offsets 0.66 meters laterally, passing by the person from point A. Whereas, when a person pays attention to the robot (right), even though he does not show a behavior of compromising to the robot after the robot's tentative actions, the high attention makes the robot realize that the person knows its existence. So it can focus on moving forward efficiently without having to take a big unnecessary detour. The final lateral offset is 0.45 meters, passing by the people from point B.

Parallel: Fig.6(b) is a more challenging version of *single* with more parallel oncoming people. The distance between people in the crowd is close, and the robot's rash advance may cause a collision. The robot must decide on whether to stop to passively avoid the human or to venture into the crowd with a high collision probability but high efficiency. When the purple person does not notice the robot (left), the robot believes that he should be given a large safety margin. However, in order to safely detour him, the planned trajectory will hit the dark blue person. So the robot would rather sacrifice its own efficiency by stopping at point C and waiting for the crowd to actively avoid it. And when the purple person pays attention to the robot (right), the robot believes he will be watchful, thus it is allowed to get closer to him without collision. This additional information makes the robot through the crowd less risky, allowing it to move forward bravely for efficiency.

C. Performance of High Efficiency in Challenging Scenarios

CG3 is compared with a classic approach TEB to illustrate its intelligence to deal with difficult scenarios.

Corridor: Fig.7(a) shows a corridor scenario, where an obstacle near the wall forms a gap that does not allow two objects to pass at the same time. When a person enters the gap, the person and the obstacle form a barrier, separating the robot and its target into two spaces. TEB fails to find a feasible path in temporal-spatial space, causing the robot to stop at A and block the corridor. Whereas, CG3 (ours) makes the robot go around the person and proactively pulls over in front of the obstacle. Before the first person (purple) enter the gap, the robot has chosen to wait at B_1. After he passes, the robot tries to enter the gap but finds the second person at this time, so it waits again at B_2 until the gap is cleared.

Overtaking: Fig.7(b) shows an overtaking scenario with a fast-walking pedestrian behind the robot. One polite option for the robot is to turn to one side to give way to the pedestrian. Besides yielding, CG3 also intelligently slows down and follows the pedestrian, who opens the way ahead so that the robot can safely follow him through the oncoming crowd, avoiding the collision risk in *parallel* scenario.

Crossing one person: Fig.7(c) shows a crossing scenario, where the robot is required to pass in front or behind the human. TEB treats humans as ordinary obstacles and finds that crossing in front of the person makes the path shorter. However, as the person moves forward, the robot is forced to follow him in order to go in front of him. CG3, on the

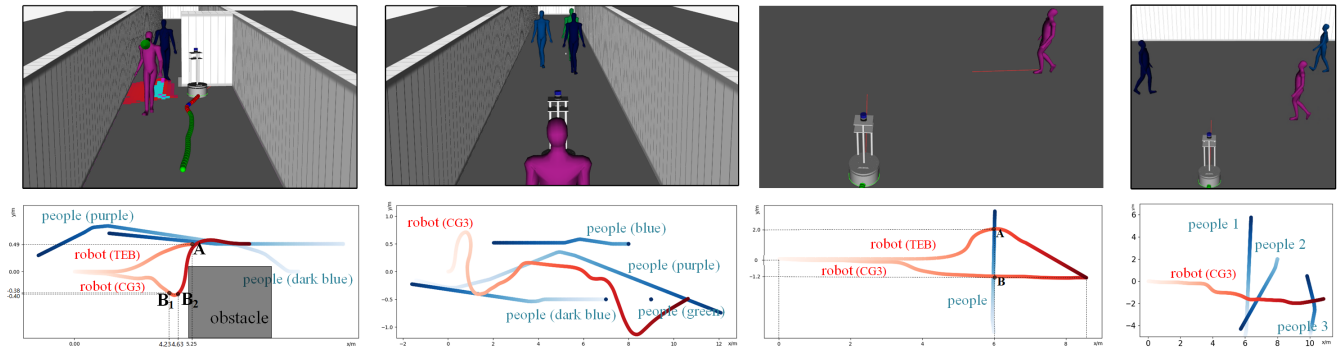

(a) Corridor with oncoming people (b) Overtaking and following (c) Crossing one person (d) Crossing three people

Fig. 7: Performance of CG3 (our approach) in challenging scenarios.

other hand, considers the relative speed of the human and the robot and detours behind the human with higher efficiency. The final time is 25.2s and 17.3s respectively.

Crossing three people: Fig.7(d) shows how the robot navigates crowds. The first person walks straight, and the robot goes behind him. The second person notices the robot and cooperates by turning right, allowing the robot to pass in front of him. The third person slows down, and the robot pass first.

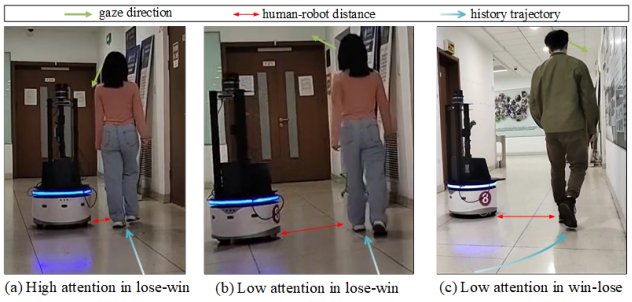

(a) High attention in lose-win (b) Low attention in lose-win (c) Low attention in win-lose

Fig. 8: Passing by people in the real world.

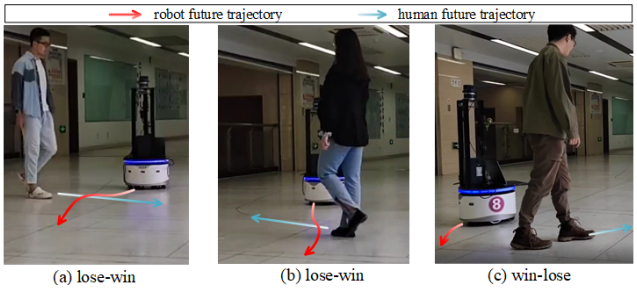

(a) lose-win (b) lose-win (c) win-lose

Fig. 9: Crossing three people in the real world.

Passing in real world: Fig.8 shows the performance of CG3 in a real-world passing scenario. The person in (a) and (b) move forward and refuse to cooperate with the robot, so the robot yields by turning right after tentative actions. It keeps a smaller distance from the person with higher attention in (a) and a larger distance from that with less attention in (b). The person in (c) cooperates with low attention, and the robot keeps a large distance from him.

Crossing in real world: Fig.9 shows the performance of CG3 in a real-world crossing scenario. When the first person refuses to cooperate, the robot goes behind him. The second one moves straight but behaves cooperatively in the relative space, allowing the robot to cooperate by turning left. The third one moves slowly. Given the relative speed and position with him, the robot turns left and tries to go in front of him. Finding the person accelerating, it switches to the right.

D. Discussion

In the above scenarios, even in the presence of sensor noise and human piece-wise steps, the robot detours stably without frequently alternating clockwise and counterclockwise due to the design of "tangent" in improved limit cycle. That is, when the game changes to *H,Win-R,Lose* situation, we actually let the robot keep the last *dir* (of *H,Lose-R,Win* or *Crash-Crash*). The redundant angles in Fig.4(a) improve the stability of decision-making. Moreover, due to limit cycle's property that does not allow objects to enter the center circle, even in the case of *H,Lose-R,win*, the robot will ensure absolute safety and obey the rules of human-centered navigation. In addition, the overtaking scenario is beyond the author's expectations. CG3 enables robots to utilize human wisdom to solve problems that cannot be solved on their own, which we think is a critical step from human-centered to human-robot collaboration.

V. Conclusion

This paper presents a human-aware navigation method CG3, and our greatest contribution is to incorporate limit cycle and human gaze information into the dynamic chicken game to model human-robot interaction. The robot estimates the safety margin for each person based on their attention to the robot, allowing the robot to pursue higher efficiency when getting more attention and to focus on safety when getting less attention. The robot can bravely and efficiently go through crowds with low collision risk. We hope CG3 can serve as a catalyst for further study. We believe that, unlike result-side information such as pose, the gaze is cause-side information, including rich information about human future intentions. How to utilize gaze information appropriately in the human-robot game would be a meaningful direction.

REFERENCES

[1] S. Lecleac'h, M. Schwager, and Z. Manchester, "Lucidgames: Online unscented inverse dynamic games for adaptive trajectory prediction and planning," *IEEE Robotics and Automation Letters*, vol. PP, pp. 1–1, 04 2021.

[2] L. A. Hayduk, "The shape of personal space: An experimental investigation." *Canadian Journal of Behavioural Science*, vol. 13, pp. 87–93, 1981.

[3] K.-C. Huang, J.-Y. Li, and L.-C. Fu, "Human-oriented navigation for service providing in home environment," in *Proceedings of SICE Annual Conference 2010*, 2010, pp. 1892–1897.

[4] C.-P. Lam, C.-T. Chou, K.-H. Chiang, and L.-C. Fu, "Human-centered robot navigation—towards a harmoniously human-robot coexisting environment," *IEEE Transactions on Robotics*, vol. 27, no. 1, pp. 99–112, 2011.

[5] L. Zhou, S. Zhang, Y. Zhao, Z. Hu, and L. Jingtai, "Modeling of personal/group dynamic comfort space based on asymmetric gaussian function," *ROBOT*, vol. 43, no. 3, pp. 257–268, 2021.

[6] P. Trautman and A. Krause, "Unfreezing the robot: Navigation in dense, interacting crowds," in *2010 IEEE/RSJ International Conference on Intelligent Robots and Systems*, 2010, pp. 797–803.

[7] T. Fischer, H. Chang, and Y. Demiris, "Rt-gene: Real-time eye gaze estimation in natural environments," in *Proceedings of the European Conference on Computer Vision (ECCV)*, 2018, pp. 334–352.

[8] H. Khalil, *Nonlinear Systems*, 3rd ed., ser. Pearson Education. Prentice Hall, 2002.

[9] D.-H. Kim and J.-H. Kim, "A real-time limit-cycle navigation method for fast mobile robots and its application to robot soccer," *Robotics and Autonomous Systems*, vol. 42, pp. 17–30, 01 2003.

[10] L. Adouane, "Orbital Obstacle Avoidance Algorithm for Reliable and On-Line Mobile Robot Navigation," in *9th Conference on Autonomous Robot Systems and Competitions*, Castelo-Branco, Portugal, May 2009.

[11] J. Vilca, L. Adouane, and Y. Mezouar, "Reactive navigation of mobile robot using elliptic trajectories and effective on-line obstacle detection," *Gyroscopy and Navigation*, vol. 4, 01 2013.

[12] L. Adouane, "Reactive versus cognitive vehicle navigation based on optimal local and global pelc," *Robotics and Autonomous Systems*, vol. 88, 11 2016.

[13] M. Kollmitz, K. Hsiao, J. Gaa, and W. Burgard, "Time dependent planning on a layered social cost map for human-aware robot navigation," in *2015 European Conference on Mobile Robots (ECMR)*, 2015, pp. 1–6.

[14] S. V. Albrecht, C. Brewitt, J. Wilhelm, B. Gyevnar, F. Eiras, M. Dobre, and S. Ramamoorthy, "Interpretable goal-based prediction and planning for autonomous driving," in *IEEE International Conference on Robotics and Automation (ICRA)*, 2021.

[15] R. Sugden, *The Economics of Rights, Cooperation and Welfare*, 2nd ed. Palgrave Macmillan, 2005.

[16] A. Rapoport and A. M. Chammah, "The game of chicken," *American Behavioral Scientist*, vol. 10, no. 3, pp. 10–28, 1966.

[17] H. Khambhaita and R. Alami, "Viewing Robot Navigation in Human Environment as a Cooperative Activity," in *International Symposium on Robotics Research (ISSR 2017)*, Puerto Varas, Chile, Dec. 2017, p. 18.

[18] Z. Zhang and J. F. Fisac, "Safe Occlusion-Aware Autonomous Driving via Game-Theoretic Active Perception," in *Proceedings of Robotics: Science and Systems*, Virtual, July 2021.

[19] Z. Wang, Y. Zhuang, Q. Gu, D. Chen, H. Zhang, and W. Liu, "Reinforcement learning based negotiation-aware motion planning of autonomous vehicles," in *2021 IEEE/RSJ International Conference on Intelligent Robots and Systems (IROS)*, 2021, pp. 4532–4537.

[20] Z. Shen, A. Elibol, and N. Y. Chong, "Understanding nonverbal communication cues of human personality traits in human-robot interaction," *IEEE/CAA Journal of Automatica Sinica*, vol. 7, no. 6, pp. 1465–1477, 2020.

[21] E. Fink, S. Gates, and B. Humes, *Game Theory Topics: Incomplete Information, Repeated Games, and N-Player Games*. Sage, 1998.

[22] M. Osborne and A. Rubinstein, *A course in game theory*. MIT press, 1994.

[23] Y. Che, A. Okamura, and D. Sadigh, "Efficient and trustworthy social navigation via explicit and implicit robot–human communication," *IEEE Transactions on Robotics*, vol. PP, pp. 1–16, 01 2020.

[24] C. Rösmann, F. Hoffmann, and T. Bertram, "Integrated online trajectory planning and optimization in distinctive topologies," *Robotics and Autonomous Systems*, vol. 88, pp. 142–153, 11 2017.

[25] H. Zhao, J. Gao, T. Lan, C. Sun, B. Sapp, B. Varadarajan, Y. Shen, Y. Shen, Y. Chai, C. Schmid, C. Li, and D. Anguelov, "Tnt: Target-driven trajectory prediction," in *CoRL*, 2020.